Analysis of Discontinuities in Planar Dielectric Waveguides: An Eigenmode Propagation Method

Qing-Huo Liu, *Member, IEEE*, and Weng Cho Chew, *Senior Member, IEEE*

Abstract—**In this paper the eigenmode propagation method is proposed to analyze the discontinuity problems in planar dielectric waveguides. This new recursive algorithm is based on the numerical mode matching method, but it uses less computation time and computer memory, which makes the analysis of multiregion, vertically stratified media much more effective. With this algorithm, the required computer memory is independent of the number of regions in the problem, and the computation time is linearly proportional to the number of regions. Therefore, it is particularly suitable for the analysis of planar waveguide discontinuities and waveguide bends. Using this method, we can analyze larger problems which are impractical with the finite element method. From the numerical examples given in the paper, it is demonstrated that the computation time is linearly proportional to the number of discontinuities, while the computer memory is almost a constant independent of the number of discontinuities, N.**

I. Introduction

BECAUSE of the importance of dielectric waveguide discontinuities in many applications in optical and millimeter-wave circuits, the analysis of these discontinuities has been of major research interest for many years [1]–[21], [24], [26], [29]–[32]. One difficulty encountered in the analysis of planar waveguide discontinuity problems is the treatment of the guided modes (or surface modes) and the radiation modes which have a continuous spectrum. Marcuse [5] derived a simple approximation for a small step at the junction of two monomode slabs. For small steps, Clarricoats and Sharpe [6] have applied the mode matching method to the discrete modes at the junction, neglecting the continuous radiation modes; Hockman and Sharpe [7] proposed the use of the first-order variational solution which neglected the backward radiation loss at the steps. A perturbation analysis of dielectric gratings was presented by Peng and Tamir [8]. For large abrupt step discontinuity cases, Mahmoud and Beal [9] have used the normalized Laguerre polynomials to expand the continuous radiation spectrum and then applied the mode-matching method to solve the problem. A mode-matching method suggested by Brooke and Kharadly [10], [20] introduces a metallic enclosure to the original waveguide structure in order to discretize the radiation spectrum. The Laguerre transform has also been used by Shigesawa and Tsuji [26] in analyzing open waveguide discontinuities. The mode-matching method used by Hosono, Hinata, and Inoue [19] approximates the waveguide structure with periodical waveguide structure in the transverse direction so as to discretize the continuous radiation modes.

In addition to the various kinds of mode matching methods, variational approaches have been applied successfully. Morishita, Inagaki, and Kumagai [13] formulated a least-squares boundary residual method with the use of a set of "proper functions" (Gauss–Laguerre functions) to transform the integral in continuous spectrum to a discrete summation. The Ritz–Galerkin (RG) variational approach has been used to analyze a step discontinuity by Rozzi [11] and subsequently to study the diffraction at the facet of a double heterostructure injection laser and a cascade of step discontinuities by Rozzi and in't Veld [14], [15]. A successive iteration Neumann series method has been proposed by Gelin *et al.* [12], [16], where the system of singular integral equations for unknown mode amplitudes is solved by iteration via the Neumann series. Suzuki and Koshiba [21] have developed a combined method in which the two-dimensional finite-element method is used for the interior region enclosing the waveguide discontinuities of arbitrary shape, while an analytical approach is used for the exterior region. Recently, Chung and Chen [29]–[31] proposed a partial variational principle for the analysis of waveguide discontinuity problems. In their method, the interior fields are also represented by finite-element nodal values, but the exterior fields are expanded as a function of the nodal values at the discontinuity region through the Green's function of the uniform slab waveguide. The advantage of this method is that in the transverse direction, the finite-element boundary can be placed very close to the discontinuity region, resulting in savings in computer resources.

In addition to the above methods, the beam-propagation method (BPM) [33]–[37] has been proposed to calculate the propagation of waveguide modes through waveguide discontinuities. Though an efficient method, the BPM is an approximate method requiring the wave to be paraxial. Furthermore, the refractive index contrast cannot be too high, and reflected waves are not accounted for. Hence, it is good only for low contrast and gradual bends in optical waveguides.

The previous methods are useful when the region of discontinuity is not very large. However, for some problems encountered in practice, the region of discontinuity is large

Manuscript received January 23, 1990; revised November 13, 1990. This work was supported by the National Science Foundation under Contract NSF ECS 85-25891, by McDonnell Douglas, and by the General Electric Company.

Q.-H. Liu was with the Department of Electrical and Computer Engineering, University of Illinois, Urbana, IL 61801. He is now with Schlumberger-Doll Research, Ridgefield, CT 06877.

W. C. Chew is with the Department of Electrical and Computer Engineering, University of Illinois, Urbana, IL 61801.

IEEE Log Number 9042341.

0018-9480/91/0300-0422$01.00 ©1991 IEEE

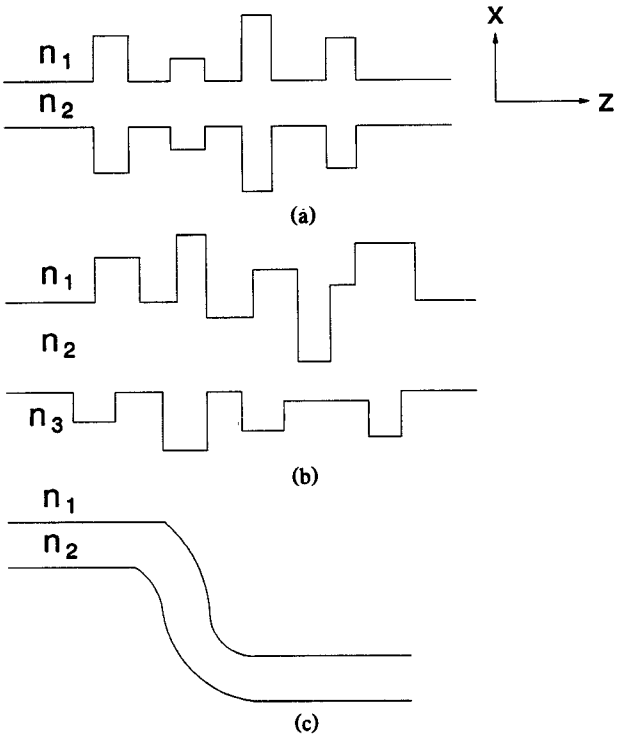

Fig. 1. Typical waveguide discontinuities studied in the paper: (a) symmetric multistep discontinuities; (b) asymmetric multistep discontinuities; and (c) waveguide misalignments and waveguide bends.

or the step discontinuities are numerous. Then these methods are ineffective in solving such problems. For the various mode matching methods, because of the large number of discontinuities, the formulation will become too laborious to carry out. While for the two-dimensional finite element method and the partial variational method, the number of unknowns required to represent the problem well will become too large. In addition, many of the above methods use PEC or PMC for the symmetric waveguide geometries in order to reduce the number of unknowns required. This will not be possible for the asymmetric waveguide geometries.

In this paper, an efficient eigenmode propagation method (EPM) is proposed to solve various problems where the discontinuity is large or the number of step discontinuities is large, as shown in Fig. 1. The eigenmode propagation method is based on the numerical mode matching method previously developed for the analysis of multiregion, vertically stratified media [38]–[40]. In Sections II and III, the theory of the eigenmode propagation method is presented. A variety of planar waveguide discontinuity problems are solved numerically in Section IV to demonstrate the use of the eigenmode propagation method.

II. Eigenmode Propagation Method

In this section, we shall describe the eigenmode propagation method (EPM). This method will account for multiple reflections in all the inhomogeneous regions. Hence, all the physics are correctly accounted for. The only approximation comes from the numerical implementation of the method.

We first consider the canonical solution of the reflection and transmission of waves by one junction discontinuity. The physics of reflection and transmission are described by reflection and transmission operators. With the solution of scattering by one junction discontinuity, we can obtain the solution to two junction discontinuities. Then a recursive algorithm can be derived such that the scattering due to $N+1$ junction discontinuities is obtained from the scattering due to N junction discontinuities. This is similar in spirit to the algorithm proposed in [41]–[43].

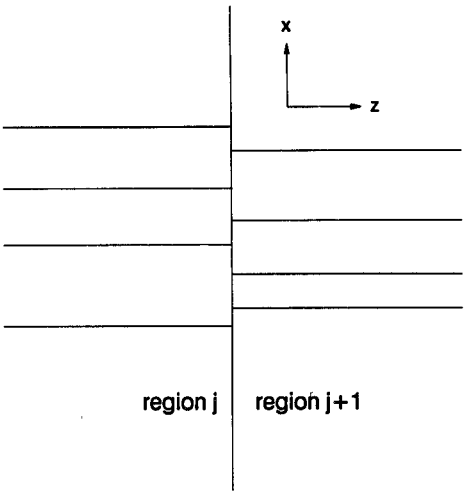

Fig. 2. A single-step discontinuity with two different layered media separated by a junction.

A. One-Junction Discontinuity Case

For simplicity, we shall illustrate the concept of EPM with the scalar wave equation. The generalization to vector wave equations can be done easily [25], [27]. Consider the single junction discontinuity shown in Fig. 2. Let us assume that the equation governing the wave propagation in this inhomogeneous medium is

$$\nabla^2\phi(\boldsymbol{r}) + k^2(\boldsymbol{r})\phi(\boldsymbol{r}) = 0 \tag{1}$$

where $k^2(\boldsymbol{r})$ is a function of position. It should be pointed out that the above equation is true only for TE waves [25]. But for the convenience of discussion, we will show only the treatment of (1) (for TE waves) in this subsection to elucidate the gist of the method. In either region of the medium shown in Fig. 2 where k^2 is independent of z, the above can be written as

$$\left[\nabla_s^2 + k^2(x,y) + \frac{\partial^2}{\partial z^2}\right]\phi(x,y)e^{\pm ik_z z} = 0 \tag{2}$$

or

$$\left[\nabla_s^2 + k^2(x,y) - k_z^2\right]\phi(x,y) = 0. \tag{2a}$$

In order to solve this equation for a uniform waveguide, we use the one-dimensional finite element method, and the unbounded waveguide structure is approximated by a bounded waveguide so as to discretize the continuous radiation spectrum (see [25], [39], [40], and [44]). With these approximations, the above can be converted into a matrix equation by letting

$$\phi(x,y) = \sum_{m=1}^{M} a_m\psi_m(x,y) \quad . \tag{3}$$

where $\psi_m(x,y)$ is some finite element basis set that can approximate $\phi(x,y)$ fairly well even when M is finite. Using (3) in (2a) and multiplying the result by $\psi_{m'}(x,y)$ and integrating over the support of $\psi_m(x,y)$, we have

$$\sum_{m=1}^{M} a_m\left[-\langle\nabla_s\psi_{m'},\nabla_s\psi_m\rangle+\langle\psi_{m'},k^2\psi_m\rangle-k_z^2\langle\psi_{m'},\psi_m\rangle\right]=0. \tag{4}$$

The above is a matrix eigenvalue problem of the form

$$\bar{\boldsymbol{L}}\cdot\boldsymbol{a}-k_z^2\bar{\boldsymbol{B}}\cdot\boldsymbol{a}=0 \tag{5}$$

where

$$[\bar{L}]_{m'm}=-\langle\nabla_s\psi_{m'},\nabla_s\psi_m\rangle+\langle\psi_{m'},k^2\psi_m\rangle \tag{6a}$$

$$[\bar{B}]_{m'm}=\langle\psi_{m'},\psi_m\rangle. \tag{6b}$$

M eigenvalues and M eigenvectors can be obtained by solving (5). The eigenfunctions can be reconstructed using (3). For example, with the αth eigenvalue and eigenvector from (5), the αth eigenfunction is

$$\phi_\alpha(x,y)=\sum_{m=1}^{M}\psi_m(x,y)a_{m\alpha}. \tag{7}$$

The general solution in region j as shown in Fig. 2 can be expanded in terms of these M eigenfunctions as

$$\phi(x,y)=\sum_{\alpha=1}^{M}\phi_\alpha(x,y)\left[e^{ik_{\alpha z}z}A_\alpha+e^{-ik_{\alpha z}z}B_\alpha\right]. \tag{8}$$

The use of vectorial notation [22], [25] allows us to write the above as

$$\phi(x,y)=\boldsymbol{\phi}^t(x,y)\cdot\left[e^{i\bar{K}_z z}\cdot\boldsymbol{A}+e^{-i\bar{K}_z z}\cdot\boldsymbol{B}\right] \tag{9}$$

where $\boldsymbol{\phi}(x,y)$ is a column vector containing $\phi_\alpha(x,y)$, $\bar{\boldsymbol{K}}_z$ is a diagonal matrix containing $k_{\alpha z}$ on the diagonal, and $\boldsymbol{A}$ and $\boldsymbol{B}$ are column vectors containing A_α and B_α respectively.

The first term in (9) is the incident wave impinging on the junction discontinuity while the second term is the reflected wave. We can define a reflection operator, $\bar{\boldsymbol{R}}_{j,j+1}$, which is the "ratio" of the reflected wave to the incident wave at $z=z_j$. Hence, the solution in region j can be formally written as

$$\phi(x,y)=\boldsymbol{\phi}_j^t(x,y)\cdot\left[e^{i\bar{K}_{jz}z}+e^{-i\bar{K}_{jz}(z-z_j)}\cdot\bar{\boldsymbol{R}}_{j,j+1}\cdot e^{i\bar{K}_{jz}z_j}\right]\cdot\boldsymbol{A}. \tag{10}$$

By the same token, the field in region $j+1$ is expressible as transmitted waves traveling in the positive z direction. We can define a transmission operator $\bar{\boldsymbol{T}}_{j,j+1}$ to express the field as

$$\phi(x,y)=\boldsymbol{\phi}_{j+1}^t(x,y)\cdot e^{i\bar{K}_{j+1,z}(z-z_j)}\cdot\bar{\boldsymbol{T}}_{j,j+1}\cdot e^{i\bar{K}_{jz}z_j}\cdot\boldsymbol{A}. \tag{11}$$

The subscripts on $\boldsymbol{\phi}^t(x,y)$ and $\bar{\boldsymbol{K}}_z$ denote that they contain the eigenfunctions and eigenvalues of the respective regions. Boundary conditions can be used to derive $\bar{\boldsymbol{R}}$ and $\bar{\boldsymbol{T}}$. For example, the continuity of the field at $z=z_j$ implies that

$$\boldsymbol{\phi}_j^t(x,y)\cdot\left(\bar{\boldsymbol{I}}+\bar{\boldsymbol{R}}_{j,j+1}\right)=\boldsymbol{\phi}_{j+1}^t(x,y)\cdot\bar{\boldsymbol{T}}_{j,j+1} \tag{12}$$

and the continuity of the normal derivative of the field at $z=z_j$ implies that

$$\boldsymbol{\phi}_j^t(x,y)\cdot\bar{\boldsymbol{K}}_{jz}\cdot\left(\bar{\boldsymbol{I}}-\bar{\boldsymbol{R}}_{j,j+1}\right)=\boldsymbol{\phi}_{j+1}^t(x,y)\cdot\bar{\boldsymbol{K}}_{j+1,z}\cdot\bar{\boldsymbol{T}}_{j,j+1}. \tag{13}$$

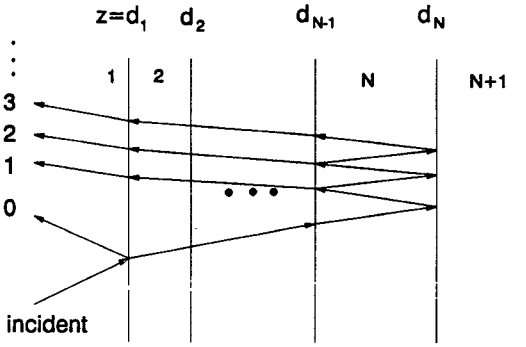

Fig. 3. Reflection field from an $N+1$-region geometry. The $N+1$-region problem is decomposed as the sum of the first N-region problem and the $(N+1)$th region. The total reflection field is the sum of all the possible multiple reflections from the first N regions and the $(N+1)$th region.

From (7), we can express $\phi^t(x,y)=\boldsymbol{\psi}^t(x,y)\cdot\bar{\boldsymbol{a}}$, where $\boldsymbol{\psi}(x,y)$ is a column vector containing $\psi_m(x,y)$ and $\bar{\boldsymbol{a}}$ is a matrix containing $a_{m\alpha}$. If the same basis is used for both regions, (12) and (13) simplify to

$$\bar{\boldsymbol{a}}_j\cdot\left(\bar{\boldsymbol{I}}+\bar{\boldsymbol{R}}_{j,j+1}\right)=\bar{\boldsymbol{a}}_{j+1}\cdot\bar{\boldsymbol{T}}_{j,j+1} \tag{14a}$$

$$\bar{\boldsymbol{a}}_j\cdot\bar{\boldsymbol{K}}_{jz}\cdot\left(\bar{\boldsymbol{I}}-\bar{\boldsymbol{R}}_{j,j+1}\right)=\bar{\boldsymbol{a}}_{j+1}\cdot\bar{\boldsymbol{K}}_{j+1,z}\cdot\bar{\boldsymbol{T}}_{j,j+1}. \tag{14b}$$

The above are matrix equations from which the matrix operators $\bar{\boldsymbol{R}}_{j,j+1}$ and $\bar{\boldsymbol{T}}_{j,j+1}$ can be found. The above derivation is easily generalized to the vector electromagnetic wave case [25], [27].

B. The Recursive Algorithm for EPM

The above shows how the reflection and transmission operators for a single interface in a two-region problem can be derived. We shall derive a recursive algorithm from which the $(N+1)$-region reflection and transmission operators can be found given the reflection and transmission operators of an N-region problem.

Given the solution of the N-region problem, the solution in region 1 can be written as

$$\phi(x,y)=\boldsymbol{\phi}_1^t(x,y)\cdot\left[e^{i\bar{K}_{1z}(z-d_1)}+e^{-i\bar{K}_{1z}(z-d_1)}\cdot\bar{\boldsymbol{R}}_{p1(N)}\right]\cdot\boldsymbol{A}. \tag{15}$$

The solution in region N is expressed as

$$\phi(x,y)=\boldsymbol{\phi}_N^t(x,y)\cdot e^{i\bar{K}_{Nz}(z-d_{N-1})}\cdot\bar{\boldsymbol{T}}_{p1(N)}\cdot\boldsymbol{A}. \tag{16}$$

In the above, $\bar{\boldsymbol{R}}_{p1(N)}$ and $\bar{\boldsymbol{T}}_{p1(N)}$ denote the generalized reflection operator and transmission operator respectively for the N-region problem when the wave is incident from region 1. The subscript p is introduced to denote the quantities for TE (to z) waves and TM (to z) waves. For TE waves, $p=h$, while for TM waves, $p=e$. In addition to $\bar{\boldsymbol{R}}_{p1(N)}$ and $\bar{\boldsymbol{T}}_{p1(N)}$, we assume that $\bar{\boldsymbol{R}}_{pN(N)}$ and $\bar{\boldsymbol{T}}_{pN(N)}$ are also known for the case where the wave is incident from region N.

When an additional $(N+1)$th region is added with a boundary at $z=d_N$, the transmitted wave in region N will be multiply reflected and transmitted. We can trace the multiply reflected wave as follows:

Consider first the case where a wave is incident from region 1. By tracing the multiply reflected wave in region N, the "ray" denoted by "1" in Fig. 3 is a consequence of the

transmitted wave in region N being reflected once by the boundary at $z = d_N$, and emerges in region 1 after passing through the "slab" region bounded by d_1 and d_{N-1}. Its amplitude is given by

$$\bar{T}_{pN(N)} \cdot \bar{P}_{pN} \cdot \bar{R}_{pN,N+1} \cdot \bar{P}_{pN} \cdot \bar{T}_{p1(N)} \cdot A \tag{17}$$

where

$$\bar{P}_{pN} = e^{i\bar{k}_{pNz}(d_N - d_{N-1})} \tag{18}$$

is the propagator matrix in region N that propagates the eigenmodes through a distance of $d_N - d_{N-1}$.

Similarly, the reflected "ray" denoted by "2" is a consequence of double reflections in region N before emerging in region 1. Its amplitude is given by

$$\bar{T}_{pN(N)} \cdot \bar{P}_{pN} \cdot \bar{R}_{pN,N+1} \cdot \bar{P}_{pN} \cdot \bar{R}_{pN(N)} \cdot \left(\bar{P}_{pN} \cdot \bar{R}_{pN,N+1} \cdot \bar{P}_{pN} \cdot \bar{T}_{p1(N)}\right) \cdot A. \tag{19}$$

By the same token, the third "ray" can be traced and so on. Consequently, the reflection operator for the $(N+1)$-region geometry incorporating multiple reflections when the wave is incident from region 1 is (see [39] and [44])

$$\bar{R}_{p1(N+1)} = \bar{R}_{p1(N)} + T_{pN(N)} \cdot \left[\bar{I} - \bar{P}_{pN} \cdot \bar{R}_{pN,N+1} \cdot \bar{P}_{pN} \cdot \bar{R}_{pN(N)}\right]^{-1} \cdot \bar{P}_{pN} \cdot \bar{R}_{pN,N+1} \cdot \bar{P}_{pN} \cdot \bar{T}_{p1(N)}. \tag{20}$$

In the above, we have finally expressed the generalized reflection operator for $(N+1)$-region geometry in terms of that for N regions and the local reflection operator $\bar{R}_{pN,N+1}$ for the junction discontinuity between regions N and $N+1$.

The generalized transmission operator $\bar{T}_{p1(N+1)}$ for the $(N+1)$-region geometry can also be expressed in terms of the generalized reflection and transmission operators for the N-region geometry and the local reflection and transmission operators for the interface of regions N and $N+1$. Similar to the analysis for the $(N+1)$-region reflection operator, the $(N+1)$-region transmission operator can be shown to be

$$\bar{T}_{p1(N+1)} = \bar{T}_{pN,N+1} \cdot \left[\bar{I} - \bar{P}_{pN} \cdot \bar{R}_{pN(N)} \cdot \bar{P}_{pN} \cdot \bar{R}_{pN,N+1}\right]^{-1} \cdot \bar{P}_{pN} \cdot \bar{T}_{p1(N)}. \tag{21}$$

Equations (20) and (21) are the recursive relations for the $(N+1)$-region generalized reflection and transmission operators when the incident wave is from region 1 in terms of the N-region generalized reflection and transmission operators. Similarly, when the incident wave is from region $N+1$, we can find the $(N+1)$-region generalized reflection and transmission operators from the N-region generalized reflection and transmission operators. The $(N+1)$-region generalized reflection operator is

$$\bar{R}_{pN+1(N+1)} = \bar{R}_{pN+1,N} + \bar{T}_{pN,N+1} \cdot \left[\bar{I} - \bar{P}_{pN} \cdot \bar{R}_{pN(N)} \cdot \bar{P}_{pN} \cdot \bar{R}_{pN,N+1}\right]^{-1} \cdot \bar{P}_{pN} \cdot \bar{R}_{pN(N)} \cdot \bar{P}_{pN} \cdot \bar{T}_{pN+1,N} \tag{22}$$

and the $(N+1)$-region generalized transmission operator is

$$\bar{T}_{pN+1(N+1)} = \bar{T}_{pN(N)} \cdot \bar{P}_{pN} \cdot \left[\bar{I} - \bar{R}_{pN,N+1} \cdot \bar{P}_{pN} \cdot \bar{R}_{pN(N)} \cdot \bar{P}_{pN}\right]^{-1} \cdot \bar{T}_{pN+1,N}. \tag{23}$$

These operators are now expressed in terms of the N-region generalized reflection and transmission operators.

The above recursive relations for the generalized reflection and transmission operators are very suitable for the analysis of slab waveguide multistep discontinuities. Starting from a two-region problem where the local reflection and transmission operators are equal to the generalized reflection and transmission operators, we can find those operators for a three-region problem by using the above relations. This procedure can be applied recursively to problems with more regions. In each step of the whole procedure, only the storage of generalized operators and that of the new local reflection and transmission operators are required. Therefore, the storage requirement is a constant independent of the number of step discontinuities. On the other hand, it is easy to see that the computation time for a multistep discontinuity problem is linearly proportional to the number of steps. This is a very important feature of this eigenmode propagation method.

III. Scattering Parameters

In the last section, we have derived the recursive relations for the generalized reflection and transmission operators which characterize the reflected field and transmitted field from a multiregion, vertically stratified medium. Using the results of previous work [25], [27], [38]–[40], these operators are easily defined for the x components of the field. Then the scattering parameters for the waveguide structure can be related to these operators.

Let us first find the scattering parameters for the TM wave [25], [27], [38]–[40] in the waveguide discontinuities. For the general slab waveguide structure shown in Fig. 1, it is assumed that the x component of the incident electric field (in region 1) is

$$D_{1x}^{(i)} = f_{e1}^t \cdot A_{e1} = S^t \cdot \bar{B}_{e1}^t \cdot A_{e1} \tag{24}$$

where A_{e1} contains the coefficients of the eigenmode expansion, f_{e1} contains the eigenmodes of region 1, and S contains the basis functions ψ_m for the eigenmodes. For the TM wave, the nonzero field components are (E_x, H_y, E_z). The y component of the magnetic field can be found from the x component of electric field:

$$H_{1y}^{(i)} = S^t \cdot \bar{H}_{e1} \cdot A_{e1} \tag{25}$$

where the matrix $\bar{H}_{e1}$ is given by

$$\bar{H}_{pj} = \omega B_{pj}^t \cdot K_{pzj}^{-1}. \tag{25a}$$

The total incident power is

$$P_{e1}^{(i)} = \frac{1}{2} \operatorname{Re} \int_{-\infty}^{\infty} \left[E_{1x}^{(i)} \cdot H_{1y}^{(i)*}\right] dx = \frac{1}{2} \operatorname{Re} \left[\langle A_{e1}^t \cdot \bar{B}_{e1} \cdot S \cdot \epsilon_1^{-1}(x) \cdot S^{\dagger} \cdot \bar{H}_{e1}^* \cdot A_{e1}^* \rangle\right] = \frac{1}{2} \operatorname{Re} \left[A_{e1}^t \cdot \bar{B}_{e1} \cdot \bar{\epsilon}_1^{-1} \cdot \bar{H}_{e1}^* \cdot A_{e1}^*\right] \tag{26}$$

where the superscript $\dagger$ denotes the complex conjugate of the transposed matrix.

For an $(N-1)$-step discontinuity (i.e., N-region) problem, the x components of the reflected and transmitted electric fields are given by

$$D_{1x}^{(r)} = \boldsymbol{S}^t \cdot \bar{\boldsymbol{B}}_{e1}^t \cdot \bar{\boldsymbol{R}}_{e1(N)} \cdot \boldsymbol{A}_{e1} \tag{27}$$

$$D_{Nx}^{(t)} = \boldsymbol{S}^t \cdot \bar{\boldsymbol{B}}_{eN}^t \cdot \bar{\boldsymbol{T}}_{e1(N)} \cdot \boldsymbol{A}_{e1} \tag{28}$$

from which the y components of the magnetic fields can be obtained:

$$H_{1y}^{(r)} = -\boldsymbol{S}^t \cdot \bar{\boldsymbol{H}}_{e1} \cdot \bar{\boldsymbol{R}}_{e1(N)} \cdot \boldsymbol{A}_{e1} \tag{29}$$

$$H_{Ny}^{(t)} = \boldsymbol{S}^t \cdot \bar{\boldsymbol{H}}_{eN} \cdot \bar{\boldsymbol{T}}_{e1(N)} \cdot \boldsymbol{A}_{e1}. \tag{30}$$

From the above, we can find the reflected power:

$$P_{e1}^{(r)} = \frac{1}{2} \operatorname{Re}\left[\boldsymbol{A}_1^t \cdot \bar{\boldsymbol{R}}_{e1(N)}^t \cdot \bar{\boldsymbol{B}}_{e1} \cdot \bar{\boldsymbol{\epsilon}}_1^{-1} \cdot \bar{\boldsymbol{H}}_{e1}^* \cdot \bar{\boldsymbol{R}}_{e1(N)}^* \cdot \boldsymbol{A}_1^* \right] \tag{31}$$

and the transmitted power:

$$P_{eN}^{(t)} = \frac{1}{2} \operatorname{Re}\left[\boldsymbol{A}_1^t \cdot \bar{\boldsymbol{T}}_{e1(N)}^t \cdot \bar{\boldsymbol{B}}_{eN} \cdot \bar{\boldsymbol{\epsilon}}_N^{-1} \cdot \bar{\boldsymbol{H}}_{eN}^* \cdot \bar{\boldsymbol{T}}_{e1(N)}^* \cdot \boldsymbol{A}_1^* \right]. \tag{32}$$

The above is for the case where the incident field is from region 1. If the incident field is from region N, it is easy to find the corresponding incident power $P_{eN}^{(i)}$, reflected power $P_{eN}^{(r)}$, and transmitted power $P_{e1}^{(t)}$. From the above equations, we can find the scattering parameters for the waveguide discontinuities for different waveguide modes. If it is supposed that the incident wave is the n_{e1}th surface mode (normalized), it is easy to show that the reflection coefficient for this mode is

$$R_{e1N} = \left[\bar{\boldsymbol{R}}_{e1(N)} \right]_{n_{e1}, n_{e1}} \tag{33}$$

and the corresponding power reflectivity is

$$r_{e1N} = |R_{e1N}|^2. \tag{34}$$

The transmission coefficient for the n_{eN}th surface mode in region N is given by

$$T_{e1N} = \sqrt{\frac{\operatorname{Re}\left(\left[\bar{\boldsymbol{K}}_{e1z} \right]_{n_{e1}, n_{e1}} \right)}{\operatorname{Re}\left(\left[\bar{\boldsymbol{K}}_{eNz} \right]_{n_{eN}, n_{eN}} \right)}} \left[\bar{\boldsymbol{T}}_{e1(N)}^t \right]_{n_{eN}, n_{e1}} \tag{35}$$

and the power transmittivity is

$$t_{e1N} = |T_{e1N}|^2. \tag{36}$$

When the incident field is from region N, we can find the corresponding reflection and transmission coefficients for the above modes as

$$R_{eN1} = \left[\bar{\boldsymbol{R}}_{eN(N)} \right]_{n_{eN}, n_{eN}} \tag{37}$$

$$T_{eN1} = \sqrt{\frac{\operatorname{Re}\left(\left[\bar{\boldsymbol{K}}_{eNz} \right]_{n_{eN}, n_{eN}} \right)}{\operatorname{Re}\left(\left[\bar{\boldsymbol{K}}_{e1z} \right]_{n_{e1}, n_{e1}} \right)}} \left[\bar{\boldsymbol{T}}_{eN(N)}^t \right]_{n_{e1}, n_{eN}}. \tag{38}$$

The above is for the scattering parameters of the TM wave. For the TE wave, these parameters can be found easily by using the duality from the above equations.

IV. Results and Applications

In this section, symmetric and asymmetric multistep discontinuities, which are particularly useful in grating couplers and distributed feedback lasers, are studied for reflectivity of the periodic corrugations of finite length. In these studies, we will assume that the waveguide material is lossless and that the waves are normally incident on the waveguide structures (i.e., $k_y = 0$). In normal incidence of the waves, there is no coupling between TE and TM waves, so the treatment of these two different polarizations can be performed separately. In the following numerical examples, the dimension of a bounded waveguide to discretize the continuous spectrum is about 30 times larger than the thickest slab, and 45 eigenmodes are used in calculation. For more detailed choice of basis functions, the reader is referred to [38].

A. Symmetric Multistep Discontinuities

The eigenmode propagation method can easily be used to analyze multistep discontinuities. For this application, we consider the periodic corrugations with finite length as shown in Fig. 4(a), which is a waveguide with symmetric multistep discontinuities. Each of the constituent corrugations is a symmetric ridge-type discontinuity. A ten-corrugation structure is studied in this paper. With $nk_0t = 1.0$, each homogeneous waveguide section can only propagate the TE_0 and TM_0 fundamental modes.

We first consider a unit-powered TE_0 mode incident from the left-hand side. Parts (a) and (b) of Fig. 4 show the reflection power $|R|^2$ and transmission power $|T|^2$ versus the period $2d$ normalized with the wavelength λ_0. As seen from Fig. 4(a), in the range of $2d/\lambda_0 = 0.30$ to $2d/\lambda_0 = 0.90$, there are many subsidiary reflection peaks in addition to the first strong reflection peak at around $2d/\lambda_0 \doteq 0.406$ and the second strong reflection peak at around $2d/\lambda_0 = 0.825$. These two strong reflection peaks correspond to the first two Bragg reflections. Between the two strong reflection peaks, there are nine subsidiary peaks (the amplitude of the ninth subsidiary peak is less than -40 dB). If the structure under consideration is infinite in length, the first Bragg reflection will occur at $2d/\lambda_0 = 0.406$, and the second Bragg reflection at $2d/\lambda_0 = 0.812$. The shift of the second Bragg reflection will diminish if the number of corrugations is increased. The reflection of the TE_0 mode by this structure is studied in [32], and a comparison of our results with those in [32] shows excellent agreement. For the sake of clarity, we do not display their result in the figure. Interested readers are referred to their paper. The transmission power versus $2d$ is shown in Fig. 4(b), where a valley occurs at $2d/\lambda_0 = 0.406$.

Next the scattering of the TM_0 mode is studied. Shown in Fig. 4(c) and (d) are the reflection and transmission powers, respectively, versus the normalized period $2d$. It is noted from Fig. 4(c) that the first strong reflection for the TM_0 surface mode appears at around $2d/\lambda_0 = 0.448$, corresponding to the first Bragg reflection of the periodic corrugation with infinite length for the TM_0 mode. The transmission power shown in Fig. 4(d) has a valley at $2d/\lambda_0 = 0.448$. The curves shown in these figures characterize the grating filter performance of the periodic corrugations with finite length. They are important in the design of various grating filters.

B. Asymmetric Multistep Discontinuities

As stated before, both the numerical method and the computer program are developed for an arbitrary number of discontinuities with arbitrary shapes. Therefore, the numerical method can be used to analyze various types of asymmet-

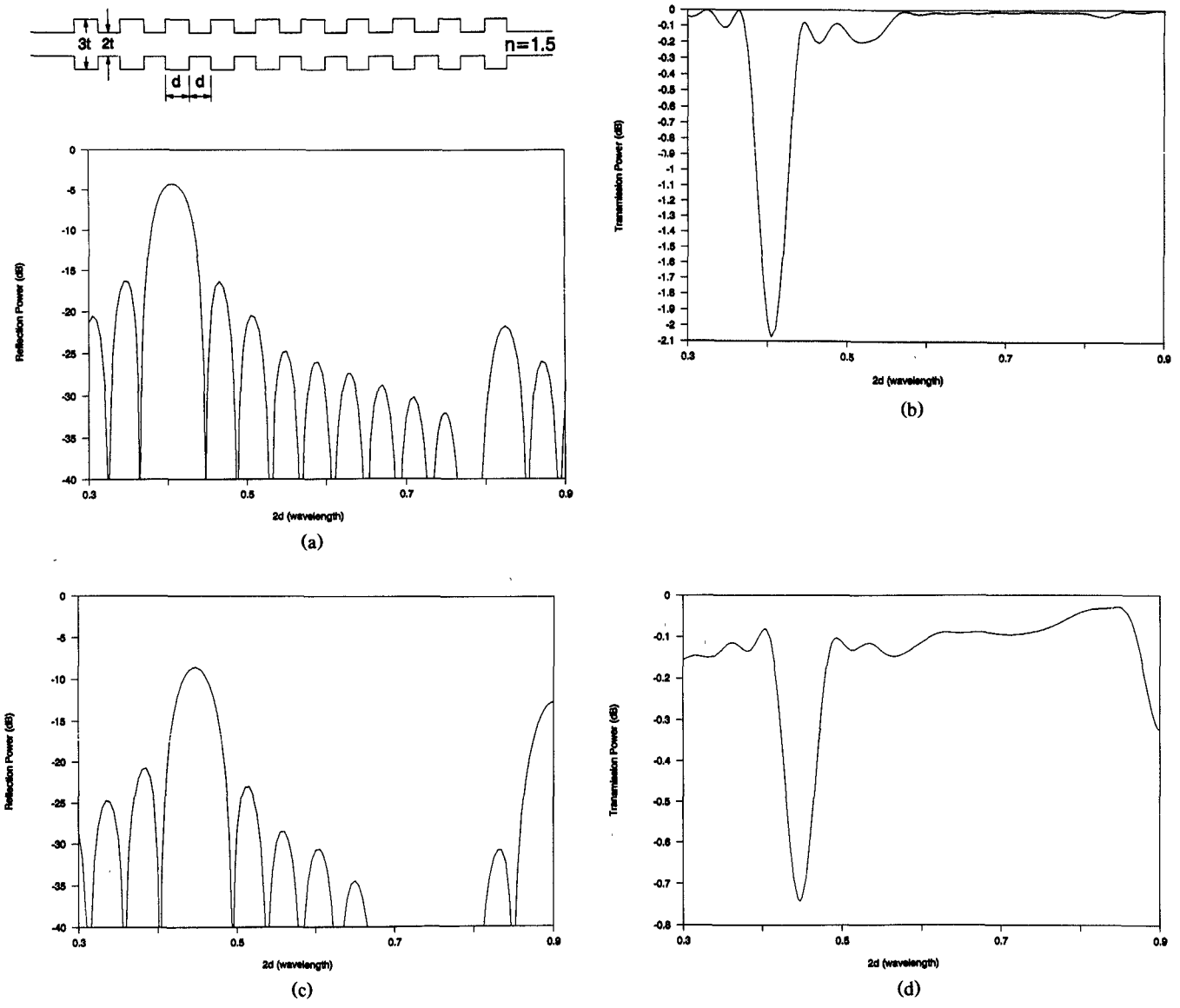

Fig. 4. Reflection and transmission powers of a symmetric multistep discontinuity with ten corrugations versus the period $2d/\lambda_0$. The parameters are $n = 1.5$ and $k_0 t = 2/3$. (a) Reflection power for the TE_0 mode. (b) Transmission power for the TE_0 mode. (c) Reflection power for the TM_0 mode. (d) Transmission power for the TM_0 mode.

ric multistep waveguide discontinuities. As a result of the interest in distributed feedback lasers, we will study asymmetric multistep discontinuities in this subsection.

We will first prove the efficiency of the eigenmode propagation method by studying the computation time and computer memory required for different numbers of discontinuities. For the asymmetric double-step discontinuity, it has been found that the first peak of the reflection coefficient for the TM_0 mode appears at about $a/d = 1.5$. Therefore, we will take the double-step discontinuity $a = 1.5d$ as a unit of the multistep discontinuity shown in the inset of Fig. 5(a). By increasing the number of units, we will study the efficiency of our algorithm and the behavior of the reflection and transmission coefficients.

Shown in Fig. 5(a) is the CPU time required for the computer program to generate the results. It is seen that the time increases linearly with respect to the number of units. It takes about 11 s on a CONVEX supercomputer for one unit; while it takes about 110 s for ten units. On the other hand, the computer storage does not change with the increase of the number of units. It is worth mentioning that since no periodic properties of the structure have been used, the computation time and the computer memory required will remain the same even if all the constituent discontinuities are different. If the periodic properties are used for the computation of the periodic structures shown in Figs. 4(a) and 5(a), the computation time will be greatly reduced. From the above results, it is seen that the EPM is very efficient, and is particularly well suited for analyzing various multistep discontinuities.

In Fig. 5(b), we show the reflection and transmission coefficients for TE_0 and TM_0 modes as functions of the number of units in the multistep discontinuity. As seen from the figure, when the number of units increases from 1 to 10, the reflection coefficient for the TE_0 mode increases to about 0.585, while that for the TM_0 mode increases to about

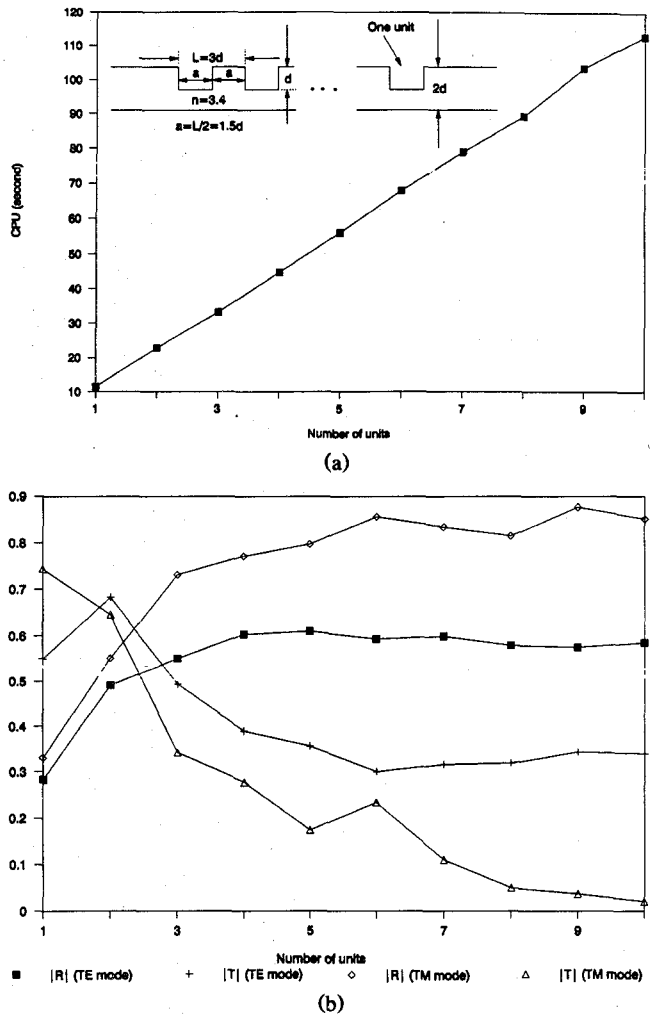

Fig. 5. An asymmetric multistep discontinuity consisting of a series of asymmetric double-step discontinuities shown in Fig. 6(b) with $a/d = 1.5$. (a) CPU time versus the number of units. (b) Amplitudes of reflection and transmission coefficients for TE_0 and TM_0 modes versus the number of units.

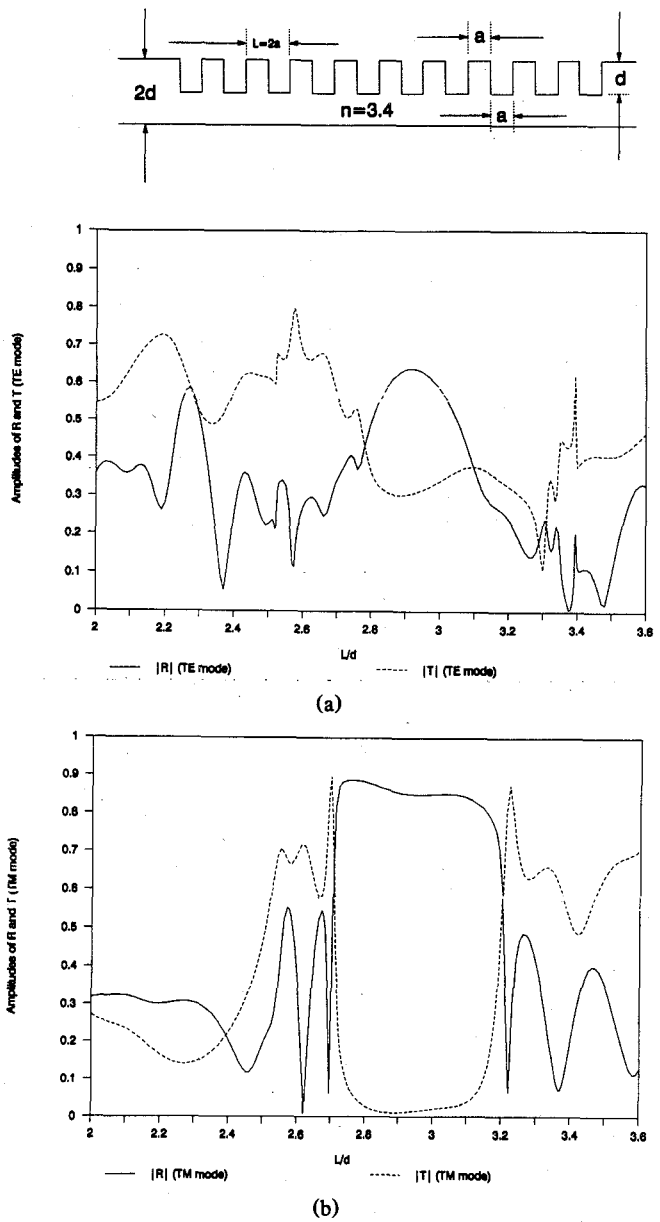

Fig. 6. Amplitudes of reflection and transmission coefficients versus the period L of a ten-unit periodic corrugation of finite length. (a) Reflection and transmission coefficients for TE_0 mode. (b) Reflection and transmission coefficients for TM_0 mode.

0.851. Meanwhile, the transmission coefficient for the TM_0 mode decreases to 0.02, and that for TE_0 decreases to 0.340.

Another problem of interest is the effect of the period L on the reflection and transmission coefficients. Shown in Fig. 6(a) is a distributed feedback laser with ten units of double steps. Different from the structure shown in the inset of Fig. 4(a), this is an asymmetric periodic corrugation of finite length. In Fig. 6(a), we show the reflection and transmission coefficients for the TE_0 mode as functions of the period L. Oscillations are observed for both curves, where a broad peak appears for the TE_0 reflection coefficient at $2.8 \leqslant L/d \leqslant 3.05$. Owing to the finite corrugation and the strong discontinuities of the problem, a rather complicated feature of the reflection and transmission coefficients occurs.

For the TM_0 mode, the reflection and transmission coefficients shown in Fig. 6(b) also have some oscillations. It is noted that when L/d increases to about 2.7, the reflection coefficient for the TM_0 mode increases sharply. In the range $2.8 \leqslant L/d \leqslant 3.1$, the reflection coefficient has a broad peak. Comparing the curves for the TE_0 mode and the TM_0 mode, one notices that the reflection and transmission coefficients for the TM_0 mode have fewer oscillations and that the main peak for the TM_0 mode is relatively flat. This kind of information is useful in designing of distributed feedback lasers and other optical components.

V. Conclusion

An efficient eigenmode propagation method (EMP) for the analysis of various discontinuities in slab dielectric waveguides has been proposed. The method is based on the numerical mode matching method for the multiregion, vertically stratified medium. The local reflection and transmission operators are used to characterize the scattering at an individual interface, while the generalized reflection and transmission operators are used to characterize the total scatter-

ing by the whole structure, which consists of several step discontinuities. The generalized reflection and transmission operators can be found using a recursive algorithm. Finally, the scattering parameters for the multistep, multimode waveguide structure are related to these generalized reflection and transmission operators. The EPM has been applied to solve a variety of slab waveguide discontinuity problems, including symmetric and asymmetric multistep discontinuities for both TE and TM incidences. It is shown that the CPU time required for the computer program is linearly proportional to the number of step discontinuities and that the storage requirement does not increase with the number of step discontinuities.

References

[1] A. F. Kay, "Scattering of a surface wave by a discontinuity in reactance," *IRE Trans. Antennas Propagat.*, vol. AP-7, pp. 22–31, 1959.

[2] C. M. Angula and W. S. C. Chang, "A variational expression for the terminal admittance of a semi-infinite dielectric rod," *IRE Trans. Antennas Propagat.*, vol. AP-7, pp. 207–212, 1959.

[3] A. D. Bresler, "On the discontinuity problem at the input to an anisotropic waveguide," *IRE Trans. Antennas Propagat.*, vol. AP-7, pp. 261–274, 1959.

[4] D. Marcuse, "Radiation losses of tapered dielectric slab waveguides," *Bell Syst. Tech. J.*, vol. 49, pp. 273–290, 1970.

[5] F. K. Reinhart, I. Hayashi, and M. Panish, "Mode reflectivity and waveguide properties of double-heterostructure injection lasers," *J. Appl. Phys.*, vol. 42, pp. 4466–4479, 1971.

[6] P. Clarricoats and A. Sharpe, "Modal matching applied to a discontinuity in a planar surface waveguide," *Electron. Lett.*, vol. 8, pp. 28–29, 1972.

[7] G. A. Hockman and A. B. Sharpe, "Dielectric waveguide discontinuities," *Electron. Lett.*, vol. 8, pp. 230–231, 1972.

[8] S. T. Peng and T. Tamir, "TM-mode perturbation analysis of dielectric gratings," *Appl. Phys.*, vol. 7, pp. 35–38, 1975.

[9] S. Mahmoud and J. Beal, "Scattering of surface waves at a dielectric discontinuity on a planar waveguide," *IEEE Trans. Microwave Theory Tech.*, vol. MTT-23, pp. 193–198, 1975.

[10] G. H. Brooke and M. M. Kharadly, "Step discontinuities on dielectric waveguides," *Electron. Lett.*, vol. 12, pp. 473–475, 1976.

[11] T. Rozzi, "Rigorous analysis of the step discontinuities in planar dielectric waveguides," *IEEE Trans. Microwave Theory Tech.*, vol. MTT-26, pp. 738–746, 1978.

[12] P. Gelin, M. Petenzi, and J. Citerne, "New rigorous analysis of the step discontinuity in a slab dielectric waveguide," *Electron. Lett.*, vol. 15, pp. 355–365, 1979.

[13] K. Morishita, S.-I. Inagaki, and N. Kumagi, "Analysis of discontinuities in dielectric waveguides by means of the least squares boundary residual method," *IEEE Trans. Microwave Theory Tech.*, vol. MTT-27, pp. 310–315, 1979.

[14] T. Rozzi and G. H. in't Veld, "Field and network analysis of interacting step discontinuities in planar dielectric waveguides," *IEEE Trans. Microwave Theory Tech.*, vol. MTT-27, pp. 303–309, 1979.

[15] T. Rozzi and G. H. in't Veld, "Variational treatment of the diffraction at the facet of d.h. laser and of dielectric millimeter wave antennas," *IEEE Trans. Microwave Theory Tech.*, vol. MTT-28, pp. 61–72, 1980.

[16] P. Gelin, S. Toutain, and J. Citerne, "Scattering of surface waves on transverse discontinuities in planar dielectric waveguides," *Radio Sci.*, vol. 16, pp. 1161–1165, 1981.

[17] M. Pudensi and L. Ferreira, "Method to calculate the reflection and transmission of guided waves," *J. Opt. Soc. Amer.*, vol. 72, pp. 126–130, 1982.

[18] K. Aoki and T. Miyazaki, "On junction of two semi-infinite dielectric guides," *Radio Sci.*, vol. 17, pp. 11–19, 1982.

[19] T. Hosono, T. Hinata, and A. Inoue, "Numerical analysis of the discontinuities in slab dielectric waveguides," *Radio Sci.*, vol. 17, pp. 75–83, 1982.

[20] G. H. Brooke and M. M. Z. Kharadly, "Scattering by abrupt discontinuities on planar dielectric waveguides," *IEEE Trans. Microwave Theory Tech.*, vol. MTT-30, pp. 760–770, 1982.

[21] M. Suzuki and M. Koshiba, "Finite element analysis of discontinuity problems in a planar dielectric waveguide," *Radio Sci.*, vol. 17, pp. 85–91, 1982.

[22] W. C. Chew, S. Barone, B. Anderson, and C. Hennessy, "Diffraction of axisymmetric waves in a borehole by bed boundary discontinuities," *Geophysics*, vol. 49, pp. 1586–1595, 1984.

[23] W. C. Chew and B. Anderson, "Propagation of electromagnetic waves through geological beds in a geophysical probing environment," *Radio Sci.*, vol. 20, pp. 611–621, 1985.

[24] C. N. Capsalis, J. G. Fikioris, and N. K. Uzunoglu, "Scattering from an abruptly terminated dielectric-slab waveguide," *J. Lightwave Technol.*, vol. LT-3, pp. 408–415, 1985.

[25] W. C. Chew, "Response of a source on top of a vertically stratified half-space," *IEEE Trans. Antennas Propagat.*, vol. AP-33, pp. 649–654, 1985.

[26] H. Shigesawa and M. Tsuji, "Mode propagation through a step discontinuity in dielectric planar waveguide," *IEEE Trans. Microwave Theory Tech.*, vol. MTT-34, pp. 205–212, 1986.

[27] W. C. Chew, "Modeling of the dielectric logging tool at high frequencies: Theory," *IEEE Trans. Geosci. Remote Sensing*, vol. 26, pp. 382–387, 1988.

[28] W. C. Chew, "Modeling of the dielectric logging tool at high frequencies: Applications and results," *IEEE Trans. Geosci. Remote Sensing*, vol. 26, pp. 388–398, 1988.

[29] S.-J. Chung and C. H. Chen, "Partial variational principle for electromagnetic field problems: Theory and applications," *IEEE Trans. Microwave Theory Tech.*, vol. 36, pp. 473–479, 1988.

[30] S.-J. Chung and C. H. Chen, "Analysis of irregularities in planar dielectric waveguide," *IEEE Trans. Microwave Theory Tech.*, vol. 36, pp. 1352–1358, 1988.

[31] S.-J. Chung and C. H. Chen, "A partial variational approach for arbitrary discontinuities in planar dielectric waveguides," *IEEE Trans. Microwave Theory Tech.*, vol. 37, pp. 208–214, 1989.

[32] H. Shigesawa and M. Tsuji, "A new equivalent network method for analyzing discontinuity properties of open dielectric waveguides," *IEEE Trans. Microwave Theory Tech.*, vol. 36, pp. 3–14, 1989.

[33] J. A. Fleck, J. R. Morris, and M. D. Feit, "Time-dependent propagation of high energy laser beams through the atmosphere," *Appl. Phys.*, vol. 10, pp. 129–160, 1976.

[34] M. D. Feit and J. A. Fleck, "Light propagation in graded-index optical fibers," *Appl. Opt.*, vol. 17, pp. 3990–3998, 1978.

[35] M. D. Feit and J. A. Fleck, "Calculation of dispersion in graded-index multimode fibers by a propagating-beam method," *Appl. Opt.*, vol. 18, pp. 2843–2851, 1979.

[36] M. D. Feit and J. A. Fleck, Jr., "Computation of mode properties in optical fiber waveguides by the propagating beam method," *Appl. Opt.*, vol. 19, pp. 1154–1164, 1980.

[37] M. D. Feit and J. A. Fleck, Jr., "Computation of mode eigenfunctions in graded-index optical fibers by the propagating beam method," *Appl. Opt.*, vol. 19, pp. 2240–2246, 1980.

[38] W. C. Chew, "Analysis of optical and millimeter wave dielectric waveguide," *J. Electromagn. Waves Appl.*, vol. 3, pp. 359–377, 1989.

[39] Q. H. Liu and W. C. Chew, "Numerical mode matching method for the multiregion vertically stratified media," *IEEE Trans. Antennas Propagat.*, vol. 38, pp. 498–506, 1990.

[40] Q. H. Liu and W. C. Chew, "Analysis of complex rectangular dielectric waveguides," *J. Electromagn. Waves Appl.*, to be published.

[41] W. C. Chew, "An N^2 algorithm for the multiple scattering solution of N scatters," *Microwave Opt. Technol. Lett.*, vol. 2, no. 11, pp. 380–383, 1989.

[42] Y. M. Wang and W. C. Chew, "An efficient algorithm for solution of a scattering problem," *Microwave Opt. Technol. Lett.*, vol. 3, no. 3, pp. 102–106, Mar. 1990.

[43] W. C. Chew and Y. M. Wang, "A fast algorithm for solution of a scattering problem using a recursive aggregate tau matrix method," *Microwave Opt. Technol. Lett.*, vol. 3, no. 5, pp. 164–169, 1990.

[44] W. C. Chew, *Waves and Fields in Inhomogeneous Media*. New York: Van Nostrand Reinhold, 1990.

✠

Qing-Huo Liu (S'88–M'89) was born in Fujian, China, on February 4, 1963. He received the B.S. and M.S. degrees, both in physics, from Xiamen University, China, in 1983 and 1986, respectively, and the Ph.D. degree in electrical engineering from the University of Illinois at Urbana–Champaign in 1989.

His research has dealt with electron paramagnetic resonance spectroscopy, microstrip antenna applications, electromagnetic wave propagation in inhomogeneous media, geophysical subsurface sensing, and transient electromagnetics. From September 1986 to December 1988, he was a Research Assistant in the Electromagnetics Laboratory at the University of Illinois, Urbana. From January 1989 to February 1990 he was a Postdoctoral Research Associate at the same Laboratory. Since March 1990 he has been a Research Scientist with Schlumberger-Doll Research, Ridgefield, CT.

Dr. Liu is a member of Phi Kappa Phi and Tau Beta Pi.

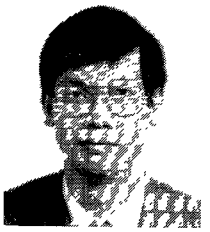

Weng Cho Chew (S'79–M'80–SM'86) was born on June 9, 1953, in Malaysia. He received the B.S. degree in 1976, both the M.S. and Engineer's degrees in 1978, and the Ph.D. degree in 1980, all in electrical engineering from the Massachusetts Institute of Technology, Cambridge.

His research has focused on wave propagation and interaction with inhomogeneous media for geophysical subsurface sensing, nondestructive testing, microwave and millimeter-wave integrated circuits, and microstrip antenna applications. He has also studied electrochemical effects and dielectric properties of composite materials. From 1981 to 1985, he was with Schlumberger-Doll Research in Ridgefield, CT, where he was a program leader and a department manager. Currently, he is a Professor in the Department of Electrical and Computer Engineering, University of Illinois at Urbana–Champaign.

Dr. Chew is a member of Eta Kappa Nu, Tau Beta Pi, and URSI and is an active member of the Society of Exploration Geophysics. He was an NSF Presidential Young Investigator for 1986. He is an Associate Editor and AdCom member of the IEEE Geoscience and Remote Sensing Society, and was a Guest Editor of the journal *Radio Science*.